

2. Temperature inside the fuel elements

Chapter 2 gives the methods for describing of the steady and of the transient temperature fields in the fuel elements. Some information is provided regarding influence of the cladding oxidation, hydrogen diffusion and of the corrosion product deposition on the temperature fields.

The fuel for the most nuclear installations used in these days is in form of small cylinders called *pellets* filled inside a closed tube called *claddings*. The closed cladding is the first barrier of the radioactivity in its way to the environment. A bundle of such tubes is called *fuel element* (in the east European countries) or *rod bundle* (in the western countries) and is prepared to be stable in transport and operation for given number of years. Groups of such bundles form the heat generating part of a nuclear reactor called *core*. Nuclear reactor cores are very complex in their material constitution design and control facilities. The heat is released with different intensity at different places of the core and varies with the time depending on the regime in which the reactor is operated. In any case something is common for all places and all times: The heat is released due to the nuclear fission inside the pellets, conducted from their volume to the gas gap and then to the cladding. Finally, the coolant is removing the heat from the surface. The subject of this section is to provide the steady state and the transient solution of the *Fourier* equation for the specific geometry of a fuel.

2.1 Steady state temperature field

Consider the geometry of the most spread type of nuclear fuel given in Fig. 2.1. The fuel radius, the gas gap thickness and the cladding thickness are R_F , δ_g , δ_C , respectively. The heat transfer coefficient at the external wall is h . This coefficient is always related to a reference coolant temperature T_{ref} . The heat released per unit volume of the fuel and unit time is \dot{q}''' . The heat has to overcome the thermal resistance to the coolant and therefore builds a temperature profile satisfying the *Fourier* equation as given in Fig. 2.1. The characteristic temperatures are: The external cladding temperature T_{s3} , the internal cladding temperature T_{s2} , the

external fuel temperature T_{s1} , and the fuel temperature at the axis of the fuel pellets T_{s0} .

Problem 1: Given the volumetric heat source that is uniform along the angle and the axis, the heat transfer coefficient and the coolant reference temperature. Compute the characteristic temperatures.

Solution: Text book solution is available for this task given below.

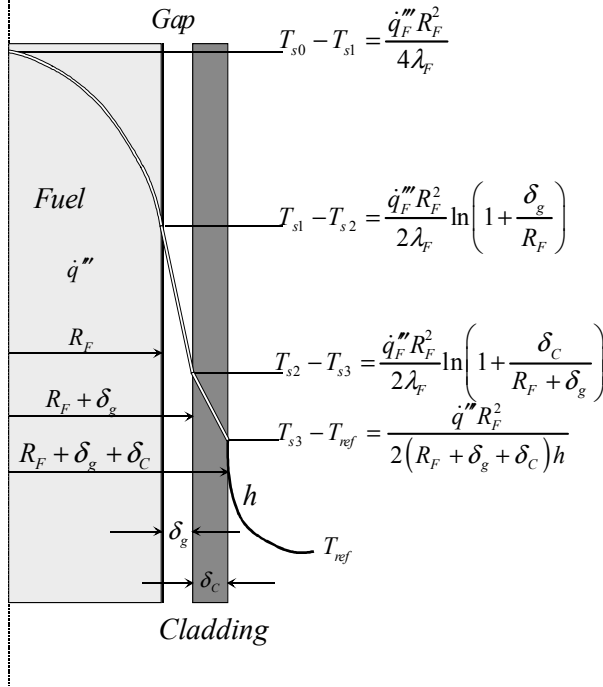


Fig. 2.1. Steady state temperature field in a fuel of nuclear reactor

Fuel: The *Fourier* equation for the cylindrical fuel is

$$\frac{1}{r} \frac{d}{dr} \left(\lambda_F r \frac{dT}{dr} \right) + \dot{q}_F''' = 0. \quad (2.1)$$

Here λ is the thermal conductivity. Its solution is

$$T(r) = -\frac{\dot{q}_F'''}{4\lambda_F} r^2 + c_1 \ln r + c_2 \quad (2.2)$$

with the boundary conditions

$$\left. \frac{dT}{dr} \right|_{r=0} = 0, \quad (2.3)$$

$$T(r=0) = T_{s0}, \quad (2.4)$$

resulting in the quadratic function

$$T(r) = T_{s0} - \frac{\dot{q}_F''' r^2}{4\lambda_F}, \quad (2.5)$$

with

$$T_{s0} - T_{s1} = \frac{\dot{q}_F''' R_F^2}{4\lambda_F}. \quad (2.6)$$

The temperature gradient at arbitrary r inside the fuel

$$\frac{dT}{dr}(r) = -\frac{\dot{q}_F''' r}{2\lambda_F}. \quad (2.7)$$

will be required in a moment. Using Eq. (2.5) we can compute the volume averaged temperature between two radiuses

$$\bar{T} = \frac{1}{\int_{r_1}^{r_2} r dr} \int_{r_1}^{r_2} r T(r) dr = T_{s0} - \frac{\dot{q}_F'''}{4\lambda_F} \frac{1}{\int_{r_1}^{r_2} r dr} \int_{r_1}^{r_2} r^3 dr = T_{s0} - \frac{\dot{q}_F'''}{8\lambda_F} (r_2^2 + r_1^2). \quad (2.8)$$

The point where it crosses the temperature profile is

$$\bar{r}_2 = \sqrt{\frac{1}{2} (r_2^2 + r_1^2)}. \quad (2.9)$$

I will use this expression by constructing the transient solution. The fuel will be divided on layers of equal volumes and the position of the averaged temperature within each layer will be postulated to be defined by Eq. (2.9).

Gas gap: The *Fourier* equation for the gas gap is

$$\frac{d}{dr} \left(r \frac{dT}{dr} \right) = \frac{d^2 T}{dr^2} + \frac{1}{r} \frac{dT}{dr} = 0. \quad (2.10)$$

Note that there is no dependence of the heat conduction of the gap. The solution of this equation is

$$T(r) = c_1 \ln \frac{r}{R_F} + c_2. \quad (2.11)$$

The boundary condition at the fuel contact surface

$$\left. \frac{dT_F}{dr} \right|_{r=R_F} = \left. \frac{dT_g}{dr} \right|_{r=R_F} \quad (2.12)$$

provides the first missing constant

$$c_1 = -\frac{\dot{q}_F'' R_F^2}{2\lambda_F}. \quad (2.13)$$

The second missing constant is provided by the boundary condition

$$T_F(R_F) = T_g(R_F), \quad (2.14)$$

Resulting in

$$c_2 = T_1. \quad (2.15)$$

Therefore the temperature as a function of the radius inside the gas gap is the quadratic function

$$T(r) = T_1 - \frac{\dot{q}_F'' R_F^2}{2\lambda_F} \ln \frac{r}{R_F}, \quad (2.16)$$

with radial temperature gradient

$$\frac{dT}{dr} = -\frac{\dot{q}_F'' R_F^2}{2\lambda_F} \frac{1}{r}, \quad (2.17)$$

which will be used in a moment. The temperature difference across the gas gap is therefore

$$T_{s1} - T_{s2} = \frac{\dot{q}_F'' R_F^2}{2\lambda_F} \ln \left(1 + \frac{\delta_g}{R_F} \right). \quad (2.18)$$

The heat flux through the gap can be expressed also in terms of the temperature difference

$$\dot{q}_{21}'' = - \frac{\lambda_g}{R_F \ln \frac{R_F + \delta_g}{R_F}} (T_{s2} - T_{s1}). \quad (2.19)$$

Note that if there is a cylinder consisting of concentric layers with left and right boundaries designated with i and $i + 1$ the heat transferred through the layers is constant in the steady state conditions.

$$\dot{Q} = - \frac{\lambda_i}{R_i \ln \frac{R_{i+1}}{R_i}} 2\pi R_i \Delta z (T_{s,i+1} - T_{s,i}). \quad (2.20)$$

The expression can be written as

$$\frac{\dot{Q}_{i,i+1}}{2\pi \Delta z} = - \frac{T_{s,i+1} - T_{s,i}}{\frac{1}{\lambda_i} \ln \frac{R_{i+1}}{R_i}} \quad (2.21)$$

with

$$R_{th,i} = \frac{1}{\lambda_i} \ln \frac{R_{i+1}}{R_i} \quad (2.22)$$

called thermal resistance. It is good exercise for the reader to prove that the heat transferred between the most left and the most right temperature is

$$\frac{\dot{Q}}{2\pi \Delta z} = - \frac{T_{s,right} - T_{s,left}}{R_{th}}, \quad (2.23)$$

where

$$R_{th} = \sum_{i=right}^{left} R_{th,i}. \quad (2.24)$$

Cladding: The procedure for the cladding is the same as the procedure for the gas gap because it is a heat conducting cylinder without internal heat sources. The solution is again

$$T(r) = c_1 \ln r + c_2 . \quad (2.25)$$

The first constant is obtained using the boundary condition

$$\left. \frac{dT_g}{dr} \right|_{r=R_F+\delta_g} = \left. \frac{dT_C}{dr} \right|_{r=R_F+\delta_g} , \quad (2.26)$$

$$c_1 = -\frac{\dot{q}_F''' R_F^2}{2\lambda_F} . \quad (2.27)$$

The second constant is obtained from the following boundary condition

$$T_g(R_F + \delta_g) = T_C(R_F + \delta_g) = T_{s2} , \quad (2.28)$$

$$c_2 = T_{s2} + \frac{\dot{q}_F''' R_F^2}{2\lambda_F} \ln(R_F + \delta_g) . \quad (2.29)$$

So finally the temperature as a function of the radius inside the cladding is

$$T(r) = T_{s2} - \frac{\dot{q}_F''' R_F^2}{2\lambda_F} \ln \frac{r}{R_F + \delta_g} . \quad (2.30)$$

The temperature difference over the cladding thickness is then

$$T_{s2} - T_{s3} = \frac{\dot{q}_F''' R_F^2}{2\lambda_F} \ln \left(1 + \frac{\delta_C}{R_F + \delta_g} \right) . \quad (2.31)$$

The external wall temperature is still unknown to close the solution. It is obtained attracting the *Newton's* heat transfer law at the surface.

Heat transfer at the surface: The heat flux at the surface is defined by

$$\dot{q}_{w \rightarrow \text{coolant}}'' = h(T_{s3} - T_{\text{ref}}) . \quad (2.32)$$

The energy conservation in steady state saying that what is generated over a fuel with axial size Δz is removed from the cladding interface over the same axial distance,

$$\dot{q}_{w \rightarrow \text{coolant}}'' \Delta z 2\pi (R_F + \delta_g + \delta_C) = \dot{q}_F''' \Delta z \pi R_F^2, \quad (2.33)$$

provides

$$\dot{q}_{w \rightarrow \text{coolant}}'' = \dot{q}_F''' \frac{R_F^2}{2(R_F + \delta_g + \delta_C)}. \quad (2.34)$$

Replacing in (2.32) results in

$$T_{s3} - T_{ref} = \frac{\dot{q}_F''' R_F^2}{2(R_F + \delta_g + \delta_C) h}. \quad (2.35)$$

A summary of the steady state solution is given in Fig. 2.1. So having a specified coolant with known temperature and velocity dictating the heat transfer coefficient all this temperatures can be computed. The relation between the heat flux and the heat inserted into unit flow is then

$$\dot{q}_{coolant}''' = \dot{q}_{w \rightarrow \text{coolant}}'' \frac{\text{Heated surface}}{\text{Flow volume belonging to this heated surface}} = \dot{q}_{w \rightarrow \text{coolant}}'' \frac{4}{D_{heat}}. \quad (2.36)$$

Here the *heated diameter* is defined generally as follows:

$$D_{heat} = 4 \frac{\text{Flow volume belonging to this heated surface}}{\text{Heated surface}}. \quad (2.37)$$

The remarkable property of this definition is that the heated diameter does not depend on the form of the channel and on the form of the heated surface.

The material temperatures are subjects to several limitations. Some of them are given in Tables 2.1 and 2.2.

Table 2.1. Upper limits for the temperatures of some fuel materials, Fratzscher and Felke (1973)

Fuel	Upper limit	°C
U	$< T_{\alpha \rightarrow \beta}$	600
UO ₂	$< T'''$	2878 ± 20
UC	$< T'''$	2370
UC ₂	$< T_{\alpha \rightarrow \beta}$	1827

Fuel	Upper limit	°C
UN	$< T'''$	2850
PuO ₂	$< T'''$	2240
ThO ₂	$< T'''$	3300

Table 2.2. Upper limits for temperatures of some cladding materials, Fratzscher and Felke (1973)

Cladding	°C	
Aluminium	150	H ₂ O
	200–300	Air
Magnesium alloys	500–550	CO ₂
Zirconium alloys	300–400	H ₂ O
Stainless steel	350–360	H ₂ O
	400–600	H ₂ O Steam
	800–900	Na

The order of magnitude of some thermal conductivities is given in Table 2.3.

Table 2.3. Thermal conductivity of some fuel and cladding materials, Fratzscher and Felke (1973)

Application	Material	Thermal conductivity in W/(mK) at 20°C
Fuel	UO ₂	5.4
	U	25.1
	22%U+Al alloy	163
	UC	29.3
	Th	37.7
	Pu	33.5 at 40°C
Cladding	Aluminum	209
	Magnesium	147
	Magnox	117
	Steel	167
	Zirconium	14.6
	Graphite	167–251

Note that the local thermal properties are functions of the local temperatures so that the obtained solutions are idealizations.

The art of designing a safe and reliable nuclear core is to select so the geometry as to guarantee in all situations the initial geometry.

2.2 Transient temperature field

Axial non-uniformity of the heat flux and angular asymmetry makes the temperature field in a fuel really three dimensional. Frequently the asymmetry is neglected and the *Fourier* equations

$$\rho c_p \frac{\partial T}{\partial \tau} - \frac{1}{r} \frac{\partial}{\partial r} \left(\lambda r \frac{\partial T}{\partial r} \right) - \frac{\partial}{\partial z} \left(\lambda \frac{\partial T}{\partial z} \right) = \dot{q}''' \quad (2.38)$$

is solved in two dimension numerically in order to describe the transient temperature fields in the fuel. The model used by myself since many years, see Kolev (1985, p. 220, 1986, p. 113, 1987, p. 108), is based on the following simplifying assumptions:

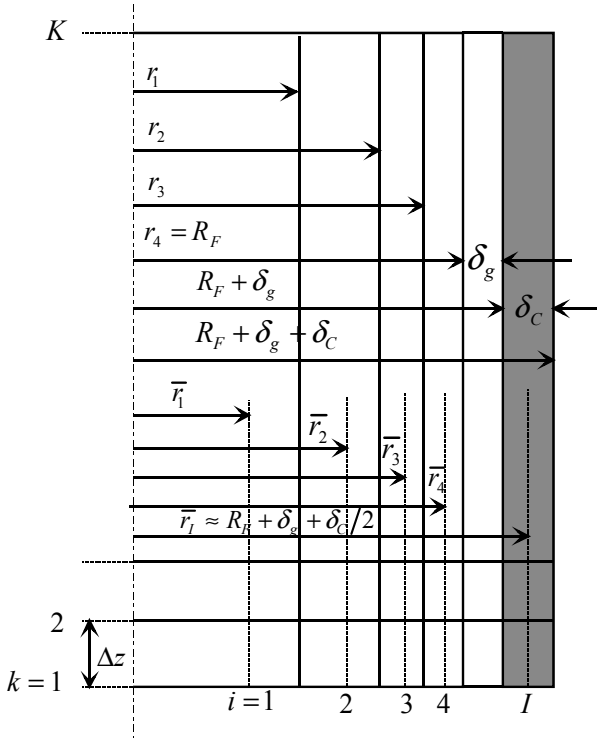


Fig. 2.2. Definition of the geometrical sizes needed for the numerical solution of the 2D-Fourier equation for nuclear reactor fuel

- The fuel is axis-symmetric: only the radial and the axial heat conduction is taken into account but not the angular;

- The gap consisting of gas does not accumulate heat because of its much lower volumetric thermal capacity ρc_p compared to the neighbouring materials;
- The thermal properties of the material are function of the local volume averaged temperature.

The computational grid is defined by I radial and K axial cells – see Fig. 2.2. The fuel has $n_F = I - 1$ cells. Each of the fuel cell has the same volume resulting in

$$r_i^2 = \frac{R_F^2 i}{n_F} \text{ for } i = 1, I - 1. \quad (2.39)$$

Note that

$$r_i^2 - r_{i-1}^2 = \frac{R_F^2}{n_F}. \quad (2.40)$$

The radius defining the position of the fuel cell averaged transient temperature

$$\bar{r}_i^2 = \frac{1}{2} (r_i^2 + r_{i-1}^2) = \frac{R_F^2 (2i - 1)}{2n_F} \text{ for } i = 1, I - 1, \quad (2.41)$$

is obtained under the assumption that the radial temperature profile at each moment remains quadratic. Indication for such assumption is given by the steady solution of the *Fourier* equation, as already mentioned before.

Using these definitions the discretized *Fourier* equation reads:

Radial cell 1:

$$(\rho c_p)_{1,k} \frac{dT_{1,k}}{d\tau} = q_{1,k}^* - \bar{\lambda}_{1,k} \frac{2}{r_1} \frac{T_{1,k} - T_{2,k}}{\bar{r}_2 - \bar{r}_1} \quad (2.42)$$

Radial cell $i = 2, I - 2$:

$$(\rho c_p)_{i,k} \frac{dT_{i,k}}{d\tau} = q_{i,k}^* + \bar{\lambda}_{i-1,k} \frac{T_{i-1,k} - T_{i,k}}{\bar{r}_i - \bar{r}_{i-1}} \frac{2r_{i-1}}{(r_i^2 - r_{i-1}^2)} - \bar{\lambda}_{i,k} \frac{T_{i,k} - T_{i+1,k}}{\bar{r}_{i+1} - \bar{r}_i} \frac{2r_i}{(r_i^2 - r_{i-1}^2)}. \quad (2.43)$$

Harmonic averaging of the thermal conductivities of the two neighbouring half layers is the natural choice here:

$$\begin{aligned}
\frac{\bar{\lambda}_{i,k}}{\bar{r}_{i+1} - \bar{r}_i} &= 2\pi r_i \Delta z \frac{2\lambda_{i,k} \lambda_{i+1,k}}{2\pi (r_i^2 - r_{i-1}^2) \Delta z \lambda_{i,k} + 2\pi (r_{i+1}^2 - r_i^2) \Delta z \lambda_{i+1,k}} \\
&= r_i \frac{2\lambda_{i,k} \lambda_{i+1,k}}{(r_i^2 - r_{i-1}^2) \lambda_{i,k} + (r_{i+1}^2 - r_i^2) \lambda_{i+1,k}}. \tag{2.44}
\end{aligned}$$

Radial cell $i = I - 1$:

$$(\rho c_p)_{i,k} \frac{dT_{i,k}}{d\tau} = q_{ik}^* + \bar{\lambda}_{i-1,k} \frac{T_{i-1,k} - T_{i,k}}{\bar{r}_i - \bar{r}_{i-1}} \frac{2r_{i-1}}{(r_i^2 - r_{i-1}^2)} - \frac{2}{(r_i^2 - r_{i-1}^2)} \frac{T_{i,k} - T_{i+1,k}}{R_{th,FC}}. \tag{2.45}$$

Here steady heat conduction is assumed in order to compute the heat flux through the three layers between the last fuel layer temperature and the cladding averaged temperature

$$\begin{aligned}
\frac{\dot{Q}_{FC}}{2\pi \Delta z} &= -\frac{T_{s1} - T_{i,k}}{\frac{1}{\lambda_{F,i,k}} \ln \frac{R_F}{\bar{r}_i}} = -\frac{T_{s2} - T_{s1}}{\frac{1}{\lambda_g} \ln \frac{R_F + \delta_g}{R_F}} = -\frac{T_C - T_{s2}}{\frac{1}{\lambda_C} \ln \frac{R_F + \delta_g + \delta_C/2}{R_F + \delta_g}} \\
&= -\frac{1}{R_{th,FC}} (T_C - T_{i,k}), \tag{2.46}
\end{aligned}$$

resulting in the definition of the effective thermal resistance

$$R_{th,FC} = \frac{1}{\lambda_{F,i,k}} \ln \frac{R_F}{\bar{r}_i} + \frac{1}{\lambda_g} \ln \frac{R_F + \delta_g}{R_F} + \frac{1}{\lambda_C} \ln \frac{R_F + \delta_g + \delta_C/2}{R_F + \delta_g}. \tag{2.47}$$

Cladding $i = I$:

$$(\rho c_p)_{i,k} \frac{dT_{i,k}}{d\tau} = q_{i,k}^* + \frac{2(T_{i-1,k} - T_{i,k})}{(r_{C,out}^2 - r_{C,in}^2) R_{th,FC}} - \frac{2(T_{i,k} - T_{coolant,k})}{(r_{C,out}^2 - r_{C,in}^2) R_{th,C}}. \tag{2.48}$$

Here steady heat conduction is assumed in order to compute the heat flux through the half of the cladding thickness

$$\frac{\dot{Q}_{FC}}{2\pi\Delta z} = -\frac{T_w - T_C}{\frac{1}{\lambda_C} \ln \frac{R_F + \delta_g + \delta_C}{R_F + \delta_g + \delta_C/2_i}} = -\frac{(T_{coolant} - T_w)}{\frac{1}{R_{C,out} h}} = -\frac{(T_{coolant} - T_C)}{R_{th,C}}, \quad (2.49)$$

resulting in a effective thermal resistance

$$R_{th,C} = \frac{1}{\lambda_C} \ln \frac{R_F + \delta_g + \delta_C}{R_F + \delta_g + \delta_C/2} + \frac{1}{R_{C,out} h}. \quad (2.50)$$

h is the heat transfer coefficient between the wall and the flow. Note that at any moment the heat flux at the wall is

$$\dot{q}_{w \rightarrow coolant}'''' = \frac{\dot{Q}_{FC}}{2\pi R_{C,out} \Delta z} = -\frac{(T_{coolant} - T_C)}{\frac{R_{C,out}}{\lambda_C} \ln \frac{R_F + \delta_g + \delta_C}{R_F + \delta_g + \delta_C/2} + \frac{1}{h}}, \quad (2.51)$$

and the external wall temperature is

$$T_w = T_{coolant} + \dot{q}_{w \rightarrow coolant}'''' / h. \quad (2.52)$$

Note also that in transients the heat produced inside the fuel is not necessarily the heat removed from the external wall by the coolant.

$$\dot{q}_{w \rightarrow coolant}'' \neq \dot{q}_F'' \frac{R_F^2}{2(R_F + \delta_g + \delta_C)}. \quad (2.53)$$

In most of the cases it is recommendable to pool the axial conduction in the term

$$q_{i,1}^* = \dot{q}_{i,1}'' + \frac{\lambda_{i,1}}{\Delta z^2} (T_{i,2} - T_{i,1}), \quad k = 1, \text{ adiabatic lower boundary}, \quad (2.54)$$

$$q_{i,k}^* = \dot{q}_{i,k}'' + \frac{\lambda_{i,k}}{\Delta z^2} (T_{i,k+1} - 2T_{i,k} + T_{i,k-1}), \quad k = 2, K-1, \quad (2.55)$$

$$q_{i,K}^* = \dot{q}_{i,K}'' + \frac{\lambda_{i,K}}{\Delta z^2} (-T_{i,K} + T_{i,K-1}), \quad k = K, \text{ adiabatic upper boundary}, \quad (2.56)$$

because it is not as strong as the radial (long slabs $L/D \gg 1$). For strong transients for instance reflood after loss of coolant accident with fast axial and temporal changes of the heat transfer coefficient in which the steam cooling is replaced fast

by water cooling, iterations are needed to resolve the thermal wave propagation with enough resolution.

For the numerical integration of the system it is convenient to write it in the following form

$$\mathbf{E} \frac{d\mathbf{T}_k}{d\tau} = \mathbf{D}_k \mathbf{T}_k + \mathbf{F}_k \mathbf{E} \quad (2.57)$$

where \mathbf{E} is the unit matrix, $\mathbf{T}_k^T = (T_{1,k}, \dots, T_{I,k})$, $\mathbf{F}_k^T = (f_{1,k}, \dots, f_{I,k})$. The components of the source vectors are

$$f_{i,k} = \frac{q_{i,k}^*}{(\rho c_p)_{i,k}}, \quad i = 1, I-1, \quad (2.58)$$

$$f_{I,k} = \frac{q_{I,k}^*}{(\rho c_p)_{I,k}} + c_{I,k} T_{coolant,k}, \quad i = I. \quad (2.59)$$

The coefficient matrix for each k is

$$\mathbf{D} = \begin{pmatrix} -c_1 & c_1 & 0 & 0 & 0 & 0 \\ b_2 & -(b_2 + c_2) & c_2 & 0 & 0 & 0 \\ 0 & b_i & -(b_i + c_i) & c_i & 0 & 0 \\ \dots & \dots & \dots & \dots & \dots & \dots \\ 0 & 0 & 0 & b_{I-1} & -(b_{I-1} + c_{I-1}) & c_{I-1} \\ 0 & 0 & 0 & 0 & b_I & -(b_I + c_I) \end{pmatrix}, \quad (2.60)$$

where the upper diagonal is

$$c_{i,k} = \frac{1}{(\rho c_p)_{i,k}} \frac{\bar{\lambda}_{i,k}}{\bar{r}_{i+1} - \bar{r}_i} \frac{2r_i}{(r_i^2 - r_{i-1}^2)}, \quad i = 1, I-2, \quad (2.61)$$

$$c_{I-1,k} = \frac{1}{(\rho c_p)_{I-1,k}} \frac{2}{(r_i^2 - r_{i-1}^2)} \frac{1}{R_{th,FC}}, \quad (2.62)$$

$$c_{I,k} = \frac{2}{(\rho c_p)_{I,k} (r_{C,out}^2 - r_{C,in}^2) R_{th,C}}, \quad (2.63)$$

and the lower diagonal is

$$b_{1,k} = 0, \quad (2.64)$$

$$b_{i,k} = \frac{1}{(\rho c_p)_{i,k}} \frac{\bar{\lambda}_{i-1,k}}{\bar{r}_i - \bar{r}_{i-1}} \frac{2r_{i-1}}{(r_i^2 - r_{i-1}^2)} = \frac{(\rho c_p)_{i-1,k}}{(\rho c_p)_{i,k}} c_{i-1,k}, \quad i = 2, I-1, \quad (2.65)$$

$$b_{I,k} = \frac{2}{(\rho c_p)_{i,k} (r_{C,out}^2 - r_{C,in}^2) R_{th,FC}} = \frac{(\rho c_p)_{I-1,k}}{(\rho c_p)_{i,k}} c_{I-1,k}, \quad (2.66)$$

Observe that the matrix is close to symmetric. It is recommendable to use explicit differentiation in the radial direction. In this case

$$\mathbf{T}_k = \left(\frac{\mathbf{E}}{\Delta \tau} - \mathbf{D}_k \right)^{-1} \left(\frac{\mathbf{T}_k^n}{\Delta \tau} + \mathbf{F}_k \right) \mathbf{E}. \quad (2.67)$$

The axial heat fluxes can be computed explicit for slow thermal transients. For fast transients iteration is necessary to update them until a solution is obtained with prescribed accuracy. The steady state solution is easily obtained writing $\Delta \tau \rightarrow \infty$,

$$\mathbf{T}_k = (-\mathbf{D}_k)^{-1} \mathbf{F}_k \mathbf{E}. \quad (2.68)$$

2.3 Influence of the cladding oxidation, hydrogen diffusion and of the corrosion product deposition

2.3.1 Cladding oxidation

Oxidation of the cladding reduces the thickness of the cladding and therefore its strength. Rassohin et al. (1971) reported that the oxidation progression with the time depends on the cladding temperature

$$M_{Zr_2O}/F = 10^{-3} \exp(-1100/T_{s3}) (\tau/3600)^{44 \exp(-1350/T_{s3})}. \quad (2.69)$$

Here M_{Zr_2O} in kg is the accumulated mass of zirconium oxide and F is the surface in m^2 on which it is build. The observations are covered with data in the region $274.15 < T_{s3} < 723.15$ K. Because the critical thickness sustaining the pressure

difference Δp of the cladding is $\delta_{C,cr} = \Delta p (R_F + \delta_g + \delta_C) / \sigma_{Zr,cr}$ where $\sigma_{Zr,cr} = 90$ to 162 MPa , the cladding oxidation reduces the strength of the cladding. The second effect is that the additional thickness of oxide possesses considerably lower thermal conductivity and presents additional thermal resistance that increases the surface temperature of the metal.

2.3.2 Hydrogen diffusion

Hydrogen is generated in nuclear reactors due to the radiolysis of water. In some plants hydrogen is additionally introduced in the water in order to reduce the content of atomic oxygen and therefore to reduce the oxidation of the structures. Rassohin et al. (1971) reported the following kinematic expression for the reached mass concentration of hydrogen in the cladding as a function of time

$$C_{H_2 \text{ in } H_2 + Zr} = \frac{D_{H_2 \rightarrow Zr}}{2\delta_C \rho_{Zr}} \frac{(\tau/3600)^{4.4 \exp(-1350/T_{Zr})}}{\exp(-1100/T_{Zr})}. \quad (2.70)$$

Here $D_{H_2 \rightarrow Zr}$ is the diffusion coefficient of hydrogen into zirconium and ρ_{Zr} is the density of the zirconium. The effect of the hydrogen is in the reduction of $\sigma_{Zr,cr}$.

2.3.3 Deposition

Depending on the water chemistry fuels standing long time in the core exhibits thin layer of corrosion products (Fe, Ca, Mg etc.) deposition. So for instance for $C_{Fe \text{ oxides}} = (0.05 \text{ to } 0.2) \times 10^{-6} \text{ kg/kg}$ can be found in some water cooled reactors, Rassohin et al. (1973). The deposition mass flow rate was reported to be function of the wall heat flux and of the mass concentration in the coolant

$$(\rho w)_{deposits} = 2.5 \times 10^{-4} \dot{q}_w'' C_{deposits} \frac{10^6}{3600}, \quad (2.71)$$

Rassohin et al. (1973). The roughness of the deposits is depending on the time of the exposition and can take values between 0.6 to $0.65 \text{ }\mu\text{m}$ up to $5 \text{ }\mu\text{m}$. The density of the deposits is reported to be very low of about 286 kg/m^3 . The heat conductivity for iron oxides is about $3.5\text{--}10 \text{ W/(mK)}$ and the heat conductivity of the other oxides (Ca, Mg etc.) can be about $3.5\text{--}35 \text{ W/(mK)}$. Therefore we have two effects of the deposits: (a) They increase the friction pressure loss because they increase the roughness; (b) They increase the thermal resistance and therefore increase the cladding temperature level.

2.4 Nomenclature

Latin

b	Coefficients
c	Coefficients
c_p	Specific capacity at constant pressure, J/(kgK)
$D_{H_2 \rightarrow Zr}$	Diffusion coefficient of hydrogen into zirconium, m ² /s
h	Heat transfer coefficient, W/(m ² K)
R_F	Fuel radius, m
$R_{C,in}$	$:= R_F + \delta_g$, inside cladding radius, m
$R_{C,out}$	$:= R_F + \delta_g + \delta_C$, outside cladding radius, m
r_i	Boundary radius of layer i , m
\bar{r}_i	Radius at which the averaged layer temperature is defined, m
T_{ref}	Fluid temperature to which the heat transfer coefficient is related, K
\dot{q}'''	Heat release per unit volume and unit time, W/m ³
T_{s0}	Fuel temperature at the axis of the fuel pellets, K
T_{s1}	External fuel temperature, K
T_{s2}	Internal cladding temperature, K
T_{s3}	External cladding temperature, K
z_k	Axial coordinate of the cell boundaries, m

Greek

$\Delta\tau$	Time step, s
Δz	Axial size of the cell, m
δ_g	Gap thickness, m
δ_C	Cladding thickness, m
λ	Thermal conductivity, W/(mK)
ρ	Density, kg/m ³
ρ_{Zr}	Density of the zirconium, kg/m ³
τ	Time, s

Subscripts

F	Fuel
C	Cladding
g	Gap
i	Layer i
k	Layer k

Superscripts

. per unit time
 ' per unit volume

References

- Fratzscher W and Felke K (1973) Einführung in die Kernenergetik, VEB Deutscher Verlag für Grundstoffindustrie, Leipzig
- Kolev NI (1985) Comparison of the RALIZA-2/02 two-phase flow model with experimental data, Nucl. Eng. Des., vol 85, pp 217–237
- Kolev NI (1986) Transiente Zweiphasenströmung (Transient Two-Phase Flow), Springer Verlag, Berlin
- Kolev NI (1987) Numerical modelling of three-phase three-component flow, Thesis for Doctor of Science Degree, Bulgarian Academy of Science, Institute for Nuclear Research and Nuclear Energy, Discipline 02.06.04 Nuclear Reactors and Nuclear Power Plants, Sofia
- Rassohin NT, Gradusov GH and Gorbatykh VP (1971) Korosija splava zirkonija – 1% niobija v uslovijah teploperedaci, Trudy MEI, Vyp. 83
- Rassohin NT, Kabanov LP, Tevlin SA and Tepsin VA (Jan. 1973) Jelesnookisnye otlojenija na teplovydeljastich poverhnostjah I ih udalenija, Preprint B-7 doklada na mejdunarodnoj konferencii po elektrohimii jidkih rastvorov pri vysokom davlenii I temperature, England

Multiphase Flow Dynamics 4

Nuclear Thermal Hydraulics

Kolev, N.I.

2009, XXXII, 745 p. 378 illus., Hardcover

ISBN: 978-3-540-92917-8